

MULTI-SENSOR BASED ADAPTIVE FUSION SCHEME FOR POSITION ESTIMATION OF MULTIROTOR UAV SYSTEMS IN GPS-DENIED ENVIRONMENTS

Luke Busse[1] & Manish Kumar[1]

[1]Department of Mechanical, Materials, and Industrial Engineering, University of Cincinnati, Cincinnati, Ohio, 45221

Abstract

The use of Uncrewed Aerial Vehicles (UAVs) has seen significant growth across a wide range of applications over the past decade. UAVs are now commonly used for outdoor tasks such as surveillance, monitoring, inspection, delivery, and aerial photography, where a Global Positioning System (GPS) is available and in most cases sufficient for localization, as large distances to obstacles make high-precision position estimation less critical. In contrast, indoor environments present a challenge for UAV localization, as GPS signals are unavailable, making reliable positioning a primary concern in such areas. This work focuses on the implementation of a novel Kalman Filter based estimation technique that delivers reliable position information to a coaxial octorotor UAV in GPS-denied environments using inexpensive LIDAR technology. Accurate position estimation of a UAV is a primary challenge for navigation in a GPS-denied environment. Use of environmentally embedded sensors (such as a motion tracking system) is a popular choice. However, their use is not feasible in many applications outside of a controlled environment. The use of onboard sensors for localization is desirable in these conditions and is an active area of research where a variety of onboard sensors, each with its own limitations and capabilities, such as LIDAR, cameras, optical flow, and other proximity sensors have been used. However, developing a robust localization method that works under a variety of operating conditions is still a challenge. The main contribution of this paper is to introduce an Adaptive Kalman Filter (AKF) framework for precise position estimation of a multirotor UAV system in GPS-denied environments solely utilizing LIDAR and Inertial Measurement Unit (IMU) technology. The LIDAR sensors used in this research include a Unitree 4D LIDAR L1 in combination with a Garmin LIDAR-Lite V3. The system was developed on a Nvidia Jetson Orin Nano and a Cube Orange Flight Controller with PX4 Autopilot software. Point-LIO 3D SLAM was used to map the environment and obtain position information. The Robot Operating System (ROS) was used for data communication between the sensors, the onboard computer, and the flight controller. Lastly, the system and its performance were validated using a high-precision OptiTrack Motion Capture system as a ground truth reference. The Root Mean Square Error (RMSE) analysis demonstrated that the fusion and predictive capabilities of the AKF algorithm significantly improved the accuracy of position estimation of the GPS-denied UAV.

Keywords: UAV, Kalman Filter, Estimation, Navigation and Control, Autonomous Vehicle

1. Introduction

Uncrewed Aerial Vehicles (UAVs) have become increasingly popular in various engineering and industrial application areas. Quadcopters, a UAV lifted by four rotors, are widely used in outdoor environments for surveillance and monitoring, inspection of construction sites or industrial facilities, delivery purposes, as well as in applications such as photography. Access to a Global Positioning System (GPS) simplifies the localization of UAVs in such conditions. Additionally, these UAVs do not usually operate in the presence of obstacles. That is why automated navigation is readily available on the market for outdoor UAVs. In indoor environments or other GPS-denied areas, this approach is not possible, which makes robust and reliable control more challenging in these surroundings.

The goal of this research is to explore and enable the application of UAVs for telehealth delivery within the homes of patients to enhance comfort and accessibility in healthcare services particularly for individuals with mobility challenges and chronic illnesses. A key technical focus of this work involves the transition from traditional outdoor UAV operation, which relies heavily on GPS, to robust and safe indoor navigation in GPS-denied environments.

Generally, UAVs suffer from natural drift caused by slight imbalances, wind disturbances, or temperature variation. This makes it difficult to safely operate them in indoor environments that are often tight and obstacle-rich spaces. Hence, reliable localization is crucial for UAV application in such areas. Additionally, this serves as a base for more intelligent operations such as autonomous waypoint navigation and can provide required stability for remote operation and obstacle avoidance.

Attempts have been made to autonomously track and localize UAVs when GPS is unavailable utilizing different methods and sensors. Visual marker approaches make use of artificial pattern-rich landmarks, such as AprilTags [1] or ArUco markers [2], that are placed in the flight area. Similarly, Bluetooth Low Energy (BLE) beacons were used to transmit position estimates to a UAV by estimating the distance between transmitter and receiver [3], which was further improved by frequency hopping techniques [4]. Ultra-Wideband (UWB) based localization is a prominent approach that makes use of a large bandwidth communication between the transmitter and receiver for distance measurements which typically also involves placement and calibration of distributed UWB devices [5][6]. Stereo cameras in conjunction with computer vision and deep learning methods were applied to estimate the pose of a UAV based on object detection algorithms [7]. Utilizing onboard computing power and interfacing precise position estimate from highly accurate motion capture camera system is another framework that was developed for indoor navigation purposes [8]. All of the aforementioned approaches are not easily transferable to different, especially unknown spaces as extensive set-up and calibration are required to make these systems functional. Onboard sensor methods have been developed utilizing cameras such as visual pose estimation where the UAV was equipped with a downward facing camera that obtained a position estimation based on special markers that were placed on the ground [9], which also required a specific setup of the room and precise calibration.

Frameworks that completely eliminate the need for external sensors and a specific configuration of the environment have focused on Simultaneous Localization And Mapping (SLAM). An example of this is the visual-inertial method where information from cameras is fused with data from an Inertial Measurement Unit (IMU). Optical flow is a popular method for velocity estimation utilizing a downward facing camera. Combined with IMU data and an additional sonar distance sensor for height estimation, optical flow based estimation has been explored in [10]. This method has the advantage of not requiring landmarks in the environment, but the ground surface must be textured for good estimation. In [11] a monocular camera was utilized to apply visual SLAM technology which provided a position estimate that was fused with data from a flight controllers IMU in an Extended Kalman Filter (EKF) framework. A similar technique was used in [12] where a microdrone was equipped with a micro IMU and onboard vision sensors.

Solutions that only rely on onboard sensing technologies provide much more flexibility and are able to utilize the full potential of UAV technology due to their capability of operating in unknown environments. LIDAR technology has been of high interest due to its reliability and performance advantage over cameras in difficult lighting conditions such as areas with insufficient illumination, sharp contrast, or when the light source is directly facing the camera lens [13]. However, the problem of higher weight and cost compared to the depth cameras, for example, often made them unattractive for indoor applications of small and lightweight UAVs [14]. RP-LIDAR, in conjunction with Hector SLAM is a widely used solution for autonomous ground vehicles and attempts have been made to transfer this technology to UAV applications in simulation [15]. Similarly, 2D LIDAR technology together with scan matching was used to improve the GPS localization of a quadcopter in urban environments [16] and areas where the GPS connection was sparse [17].

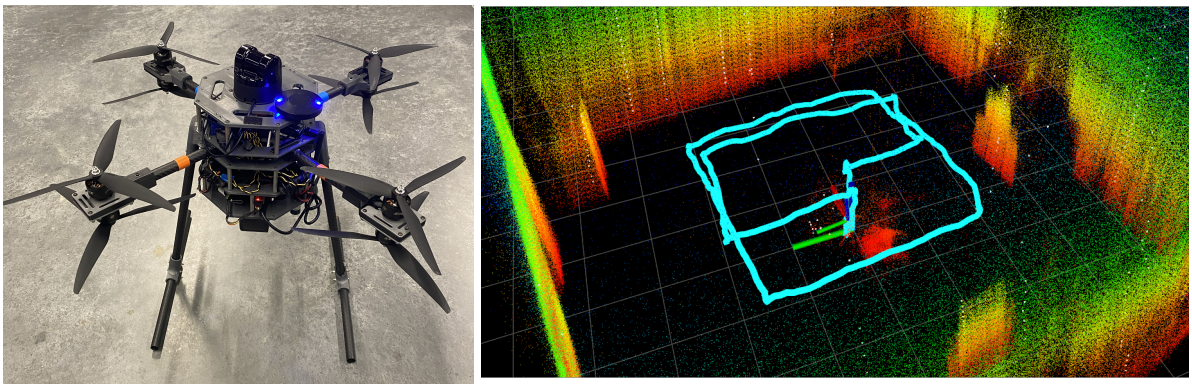
We have found that real-world implementation varies significantly from simulation results due to the environmental effects caused by noise and disturbances. For example, a simulation of accurate position control of a multirotor UAV utilizing two-dimensional sensor technology (RP-LIDAR) together with Hector SLAM for x and y control and a one-dimensional LIDAR for height control is easily attainable.

However, replicating a stable system using these sensors in a real-world experiment can be difficult due to the significant and very rapid drift of the UAV indicating that position control in the x-direction and y-direction is very imprecise. Thus, the primary objective of this paper is to develop a sensor fusion scheme that makes use of multiple sensors including a 3D LIDAR to overcome this challenge. In particular, we utilized a combination of inexpensive LIDAR sensors and IMU sensors to obtain precise local position information. In addition to their insensitivity to lighting conditions, LIDAR sensors are well-suited for simple integration with active obstacle avoidance and path planning systems, as they provide fast and accurate distance measurements to surrounding objects. This makes LIDAR an excellent choice for the purposes of this research. Extending the localization framework with automated path planning and avoidance of obstacles is particularly helpful in ensuring safe and reliable UAV navigation in indoor environments, but does not represent the primary contribution and hence is not further discussed for the purpose of this work and is addressed in an additional contribution.
The main focus of this paper is the development of an adaptive and asynchronous, real-time filtering approach based on a Kalman Filter that combines sensor information from a one-dimensional Garmin LIDAR-Lite V3, Unitree 4D LIDAR L1, and an IMU. The Unitree sensor has distinct advantages over other three-dimensional LIDAR sensors available on the market as it is more cost-effective and significantly lighter making it more suitable for UAV applications. The sensor provides position measurement in a three-dimensional space x, y, and z, and also a one-dimensional gray scale as its fourth dimension. For the purpose of this work, we disregarded the gray scale and only utilized the position measurement capabilities of the sensor. For the remainder of this paper, we will refer to this sensor as being three-dimensional. Additionally, it spins bidirectional in a 360° x 180° range, which creates a semi-spherical map of the environment while other available 3D LIDAR technology only spin in a unidirectional 360° range and output a cone of rays which ultimately creates a torus shaped map. As a result, the sensor of our choice creates much higher vibrations causing the entire system to shake once rigidly mounted. A vibrating 3D LIDAR system performs poorly in creating 3D point clouds and can lead to erroneous estimations. Traditional control systems experience estimation inaccuracies when the noise level is time-varying. For example, in a Kalman Filter the covariance matrices must be tuned to allow convergence [18]. Adaptive methods can provide more accurate noise characteristics so that the estimation in vibration intensive environments can be improved, which is important for GPS-denied flight operations. Hence, we developed an adaptive control system that is able to manage the vibrations produced from the experimental UAV with LIDAR and output a robust and precise position estimate.
We verified our results using a highly accurate motion capture system that utilized 16 cameras and obtained measurements with a recorded accuracy of 0.3 millimeters. We used these measurements as our ground truth and calculated the Root Mean Square Error (RMSE) from the local position estimate of the UAV with respect to the motion capture measurement to precisely determine how close our position estimate is to the real location in space. Additionally, we implemented fully autonomous flight capabilities based on human defined waypoints that can either be defined before flight as a mission protocol or during flight utilizing the map created by SLAM.

2. Methodology

2.1 Hardware Design

We developed a hardware architecture tailored for the integration of 3D LIDAR and telehealth technology into our small UAV system following the specific requirements of indoor flight. It uses a coaxial octorotor configuration, that provides robustness and high lift capabilities of over five kilograms, able to accommodate the onboard sensors and computational intelligence, as well as additional payload for medical purposes. In Fig. 1a, the UAV that we have developed and used for this study can be seen. To maintain maneuverability in indoor environments, the UAV is compact, with dimensions of 63 centimeters in both width and length. We utilize PX4, an open-source flight software widely used in multirotors in both research and industrial applications, in conjunction with a Cube Orange flight controller which is known for its versatility and reliability, making it suitable for a wide range of UAV applications. Additionally, the UAV is equipped with a Nvidia Jetson Nano Orin for high-performance onboard computing that enables real-time data processing from sensors using the developed Kalman



(a) Experimental Coaxial Octorotor UAV (b) SLAM output image

Figure 1 – Experimental UAV and LIDAR environment output

Filter scheme and provides the ability to host telehealth sessions. Fig. 1b shows an exemplary SLAM output map with a demonstration of the experimental flight trajectory. This image visualizes the sparsely populated test environment, which included a set of three boxes (on the right, bottom, and left of image) and a table (top right) to introduce small features and provide distance references. Here it can be seen, that our developed approach ensures stable localization even in environments with few features and obstacles, which is traditionally a challenge faced by LIDAR-SLAM algorithms.

2.2 Adaptive position estimation method

To fuse data from different sensors, we utilize a Kalman Filter approach which is widely accepted in sensor fusion and state estimation. Equation (1) represents the state $\mathbf{x}_k \in R^n$ of our system. To fully define the current local position and orientation in space with respect to the takeoff location, n is equal to ten in our scenario, defined through the three-dimensional position and velocity in the x-, y-, and z-direction as well as by its orientation in quaternions represented by q_{0_k}, q_{1_k}, q_{2_k}, and q_{3_k}.

$$\hat{\mathbf{x}}_k = \begin{bmatrix} x_k & y_k & z_k & \dot{x_k} & \dot{y_k} & \dot{z_k} & q_{0_k} & q_{1_k} & q_{2_k} & q_{3_k} \end{bmatrix}^T \tag{1}$$

The Kalman Filter equations are provided below:

$$\hat{\mathbf{x}}_{k|k-1} = F_k \hat{\mathbf{x}}_{k-1|k-1} + B_k \mathbf{y}_{1_{k-1}} + \frac{1}{2}\Delta t \mathbf{y}_{2_{k-1}} \otimes q_{k-1} \tag{2}$$

$$P_{k|k-1} = F_k P_{k-1|k-1} F_k^T + Q_{k-1} \tag{3}$$

$$K_k = P_{k|k-1} H_k^T (H_k P_{k|k-1} H_k^T + R_k)^{-1} \tag{4}$$

$$\hat{\mathbf{x}}_{k|k} = \hat{\mathbf{x}}_{k|k-1} + K_k(z_k - H_k \hat{\mathbf{x}}_{k|k-1}) \tag{5}$$

$$P_{k|k} = (I - K_k H_k) P_{k|k-1} \tag{6}$$

Here, k represents the time step, $P_{k|k} \in R^{(n \times n)}$ is the error covariance matrix representing the uncertainty of our state estimates. It may be noted that the filter represented in (2) - (6) utilizes the measurements from two sensors: A 3D LIDAR (that provides 3D positional measurement) and a 1D LIDAR (that provides 1D height (along the z-axis) measurement). $F_k = I^{(n \times n)}$ is defined as an identity matrix for incoming data from both the 3D LIDAR and the 1D LIDAR. The observation matrix H is dependent on the received sensor measurement. In the case that the data is obtained from the 3D LIDAR, H is a matrix of size $n \times n$, shown in (7), defining position and orientation as part of the measurement $\mathbf{z}_k$. This measurement relates to the odometry data that is obtained from SLAM, which provides information about the current position in x, y, and z as well as angular orientations. H reflects these measurements such that velocity and the quaternion values of the state are directly updated from the received sensor data. When readings from the one-dimensional distance sensor are

received, H is defined to be of size $1 \times n$ as presented in (8) because only position along the z-axis, z_k, is part of the measurement $\mathbf{z}_k$ and is therefore directly updated within the state of the system.

$$H_{k_{3D}} = \begin{bmatrix} 1 & 0 & 0 & 0 & 0 & 0 & 0 & 0 & 0 & 0 \\ 0 & 1 & 0 & 0 & 0 & 0 & 0 & 0 & 0 & 0 \\ 0 & 0 & 1 & 0 & 0 & 0 & 0 & 0 & 0 & 0 \\ 0 & 0 & 0 & 0 & 0 & 0 & 0 & 0 & 0 & 0 \\ 0 & 0 & 0 & 0 & 0 & 0 & 0 & 0 & 0 & 0 \\ 0 & 0 & 0 & 0 & 0 & 0 & 0 & 0 & 0 & 0 \\ 0 & 0 & 0 & 0 & 0 & 0 & 1 & 0 & 0 & 0 \\ 0 & 0 & 0 & 0 & 0 & 0 & 0 & 1 & 0 & 0 \\ 0 & 0 & 0 & 0 & 0 & 0 & 0 & 0 & 1 & 0 \\ 0 & 0 & 0 & 0 & 0 & 0 & 0 & 0 & 0 & 1 \end{bmatrix} \tag{7}$$

$$H_{k_{1D}} = \begin{bmatrix} 0 & 0 & 1 & 0 & 0 & 0 & 0 & 0 & 0 & 0 \end{bmatrix} \tag{8}$$

At a given time k when data from a LIDAR sensor is obtained we combine this measurement with IMU data in the Prediction or Process Equation (2) as a control input. The measurements of the IMU are divided into two parts, the first corresponds to the positional information and the second to the orientation of the UAV. The position part is defined by the linear acceleration measurement $\mathbf{y}_{1_{k-1}}$ in (9) and is related to the position and velocity states based on the time interval Δt shown in (10). Here, B_k is a matrix of size $n \times 3$ to relate to the linear acceleration along the x, y, and z axes. The orientation part comprises of the angular velocity values from the IMU - p, r, and s. The prediction equation (2) uses quaternion multiplication of angular velocity with the quaternion of the previous timestep q_{k-1}, shown in Equation (11), for updating the quaternion values. We utilized quaternion multiplication denoted by $\otimes$ in (2) [19] in a simplified manner assuming the bias of the measured data to be zero. Equation (12) demonstrates the applied quaternion multiplication method. Similarly to the linear control input, the size of $\mathbf{y}_{2_{k-1}}$ is directly dependent on the quaternion matrix q_{k-1} and hence of size $n \times 4$. After the measurement update in the Kalman Filter, the quaternion in the state is normalized to ensure a unit quaternion is published in ROS to be communicated with PX4.

$$\mathbf{y}_{1_{k-1}} = \begin{bmatrix} a_{x_{k-1}} \\ a_{y_{k-1}} \\ a_{z_{k-1}} \end{bmatrix} \tag{9}$$

$$B_k = \begin{bmatrix} \frac{1}{2}\Delta t^2 & 0 & 0 \\ 0 & \frac{1}{2}\Delta t^2 & 0 \\ 0 & 0 & \frac{1}{2}\Delta t^2 \\ \Delta t & 0 & 0 \\ 0 & \Delta t & 0 \\ 0 & 0 & \Delta t \\ & \mathbf{0}_{4\times 3} & \end{bmatrix} \tag{10}$$

$$q_{k-1} = \begin{bmatrix} q_{0_{k-1}} & q_{1_{k-1}} & q_{2_{k-1}} & q_{3_{k-1}} \end{bmatrix}^T \tag{11}$$

$$\mathbf{y}_{2_{k-1}} \otimes q_{k-1} = \begin{bmatrix} & & \mathbf{0}_{6\times 4} & \\ 0 & -p & -r & -s \\ p & 0 & s & -r \\ r & -s & 0 & p \\ s & r & -p & 0 \end{bmatrix}_{k-1} \begin{bmatrix} q_0 \\ q_1 \\ q_2 \\ q_3 \end{bmatrix}_{k-1} \tag{12}$$

The process noise covariance Q and the observation covariance matrix R for the 3D LIDAR are continuously updated using equations (13) and (14) respectively to directly relate the vibration noise

present in the system to the state estimates calculated in the filter.

$$Q_{k_{3D}} = \begin{bmatrix} c_q|a_{x_i}| & 0 & 0 & 0 & 0 & 0 & 0 & 0 & 0 & 0 \\ 0 & c_q|a_{y_i}| & 0 & 0 & 0 & 0 & 0 & 0 & 0 & 0 \\ 0 & 0 & c_q|a_{z_i}| & 0 & 0 & 0 & 0 & 0 & 0 & 0 \\ 0 & 0 & 0 & 1 & 0 & 0 & 0 & 0 & 0 & 0 \\ 0 & 0 & 0 & 0 & 1 & 0 & 0 & 0 & 0 & 0 \\ 0 & 0 & 0 & 0 & 0 & 1 & 0 & 0 & 0 & 0 \\ 0 & 0 & 0 & 0 & 0 & 0 & 1 & 0 & 0 & 0 \\ 0 & 0 & 0 & 0 & 0 & 0 & 0 & 1 & 0 & 0 \\ 0 & 0 & 0 & 0 & 0 & 0 & 0 & 0 & 1 & 0 \\ 0 & 0 & 0 & 0 & 0 & 0 & 0 & 0 & 0 & 1 \end{bmatrix} \tag{13}$$

$$R_{k_{3D}} = \begin{bmatrix} c_{1_r}|a_{x_i}| & 0 & 0 & 0 & 0 & 0 & 0 & 0 & 0 & 0 \\ 0 & c_{1_r}|a_{y_i}| & 0 & 0 & 0 & 0 & 0 & 0 & 0 & 0 \\ 0 & 0 & c_{2_r}|a_{z_i}| & 0 & 0 & 0 & 0 & 0 & 0 & 0 \\ 0 & 0 & 0 & 1 & 0 & 0 & 0 & 0 & 0 & 0 \\ 0 & 0 & 0 & 0 & 1 & 0 & 0 & 0 & 0 & 0 \\ 0 & 0 & 0 & 0 & 0 & 1 & 0 & 0 & 0 & 0 \\ 0 & 0 & 0 & 0 & 0 & 0 & 1 & 0 & 0 & 0 \\ 0 & 0 & 0 & 0 & 0 & 0 & 0 & 1 & 0 & 0 \\ 0 & 0 & 0 & 0 & 0 & 0 & 0 & 0 & 1 & 0 \\ 0 & 0 & 0 & 0 & 0 & 0 & 0 & 0 & 0 & 1 \end{bmatrix} \tag{14}$$

Here, c_q, c_{1_r}, and c_{2_r} are constant values that are tuned based on flight performance. c_{2_r} is used so that lower trust is given to the measurement of the 3D LIDAR in the z-direction and our estimate relies more on the distance sensor for height estimation, as the measurement of the 1D LIDAR is expected to significantly outperform the 3D LIDAR along this axis. It might also be noted, that the linear acceleration values are averaged over twenty frames to obtain a_x, a_y, and a_z in time period **i**. This is achieved using the much higher data rate of the IMU compared to the output of the SLAM algorithm and the 1D LIDAR measurements respectively with the aim to avoid extreme acceleration values affecting the localization estimate and possibly causing instability.

2.3 System Architecture

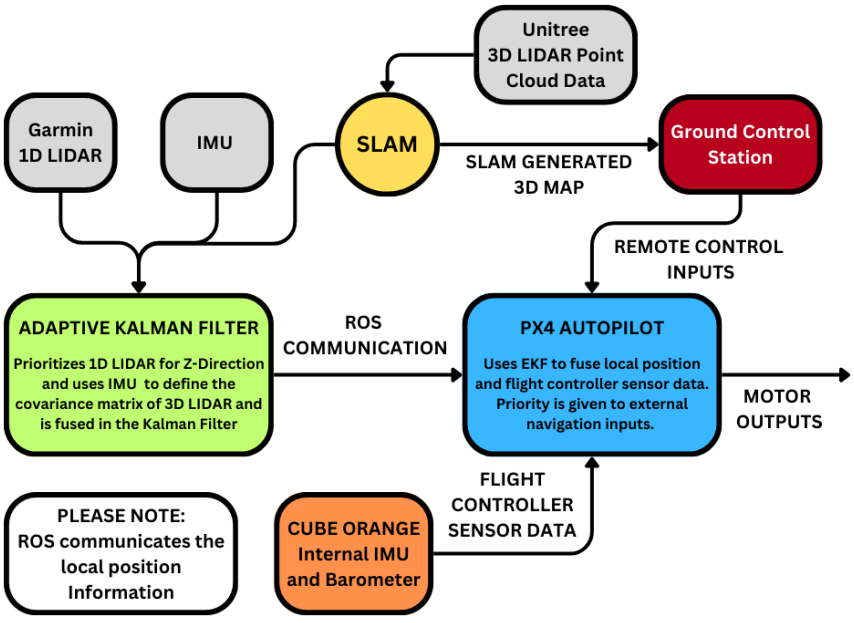


Figure 2 – Estimation and Control System Architecture

The system architecture of our UAV, shown in Fig. 2, is built on multiple sensors providing data to the adaptive estimation algorithm to enable accurate position control. The 3D LIDAR feeds data into Point-LIO (LIDAR-Inertial Odometry) 3D SLAM algorithm [20] which generates a detailed spatial map of the environment and tracks the UAVs position within it. In the Kalman Filter, the output from the SLAM is combined with additional sensor data from a 1D LIDAR and IMU. Vibrations introduced by both the 3D LIDAR and the UAV itself can cause significant noise and uncertainty in the sensor measurements. Hence we adjust the covariance dynamically based on real-time observations making the Kalman Filter adapt to noise levels of the system.
The state estimates from the Kalman filter are communicated through Robot Operating System (ROS) to PX4, which utilizes an Extended Kalman Filter (EKF) itself to further integrate this information with data from the IMU's of the Cube Orange flight controller. PX4 architecture utilizes two distinct parts for state estimation, where 24 states define angular orientation, position, velocity, IMU and Magnetometer Bias, Magnetic Field, and Wind. The EKF state estimator is used to obtain a first prediction of the current state based in inertial navigation calculations from the inbuilt IMU of the flight controller. This initial state is then updated with data obtained from other sensors to refine the estimation. In this step we fuse the output of our AKF algorithm into the estimation model of PX4. To further improve the accuracy and stability of our approach we have modified the EKF of PX4 by associating higher noise values to the IMU's of the flight controller to reduce the extent to which the estimator relies on this data and increase the trust into the provided position estimate from our fusion scheme. PX4 combines its EKF with an output prediction algorithm that accounts for the time delay in the system. Here it should be noted, the distinction between our developed AKF approach is distinct from the EKF state estimator from PX4. This allows optimized processing on the Nvidia Jetson as well as individual tuning of the Kalman Filter parameters to improve the state estimation accuracy. Hence, PX4 treats the state of our sensor fusion as local position information, which can be leveraged in two key ways: for fully indoor flight by defining a user-specified local origin as the reference start point, or for seamless transition from outdoor to indoor environments by initially relying on GPS for global positioning and then continuously updating the UAV's estimated global coordinates using relative changes from the local position data as it moves into GPS-denied areas.
PX4 then further translates this information into control signals to dictate the speed of each motor. Additionally, a SLAM-generated map is sent to the ground control station for visualization of the UAVs surroundings to enable remote operation or track the progress of autonomous missions.

3. Experimentation

To validate the effectiveness of the proposed control scheme, we conducted a series of experiments. First, we performed a specified mission test outdoors with the aid of GPS to obtain baseline information about the performance of the experimental UAV platform. Due to the deteriorated performance of LIDAR outdoors, we included GPS in this test. Successively, we transitioned to an indoor environment with GPS unavailable and tested our control approach by incrementally integrating sensor technology and adaptive filtering algorithms into the UAVs navigation system. Each experiment involved flying the drone with continuous motion in a square pattern for approximately one minute, with both the takeoff and landing locations marked at the center of the square. We performed multiple flights for each individual sensor setup and averaged the obtained results to ensure statistical reliability of the presented data.
In Experiment 1, we merely utilized the 3D LIDAR in conjunction with Point-LIO 3D SLAM algorithm. The data generated by the LIDAR was sent directly to the the EKF of PX4, allowing us to assess its performance based solely on this information to establish a baseline for our proposed approach.
In Experiment 2, we added a Garmin 1D LIDAR sensor to the system. We modified the PX4 EKF configuration to rely on distance sensor information for height reference to demonstrate the importance of highly precise data in the z-direction for stable and reliable flight operation.
In Experiment 3, we incorporated real-time state estimation and prediction by implementing a Kalman Filter on the onboard computer to combine data from both the 3D LIDAR and 1D LIDAR. Similarly to Experiment 1, PX4's EKF was updated to rely entirely on the external position estimate. The Kalman Filter optimizes state estimation by reducing the impact of measurement noise, allowing for smoother and more reliable position information during flight.

Finally, in Experiment 4, we enhanced the Kalman Filter by making the covariance matrices dependent on the vibrations measured by the IMU sensor allowing the Kalman Filter to become adaptive. With this we expected significant improvements in the estimation accuracy by integrating acceleration data into both our noise model and measurement equation as the vibration noise level experienced by the UAV is high and inconsistent, and is expected to adversely affect the 3D LIDAR data.
To validate our results, we utilized a high-accuracy OptiTrack Motion Capture system comprised of 16 cameras that were calibrated with an accuracy of 0.3 millimeters. The obtained results from the system were treated as a ground truth reference for the flight experiments. This setup enabled us to detect seven markers on the UAV and calculate the error between the local position estimates (Obtained from the AKF/SLAM/PX4) and the true location captured by the motion capture system. By comparing these values across the different experimental setups, we aimed to demonstrate the effectiveness of our control scheme in real-world conditions.

4. Results

To evaluate our proposed approach, we utilized the local position information obtained from the flight logs of PX4 and compared the values relative to each axis of motion with the ground truth data obtained from the OptiTrack Motion Capture system mentioned previously. We utilized Root Mean Square Error (RMSE) as the metric of comparison to demonstrate the average error over time. To apply this metric, we first initialized values for x, y, and z to align the measurements from the motion capture system and the local position estimate. Fig. 3 depicts an example of the manual control inputs provided during a fully autonomous flight test. Here, it can be seen, that the UAV operates in the autonomous modes mission and return to land (RTL) so that manual control inputs from the pilot are not needed during flight.

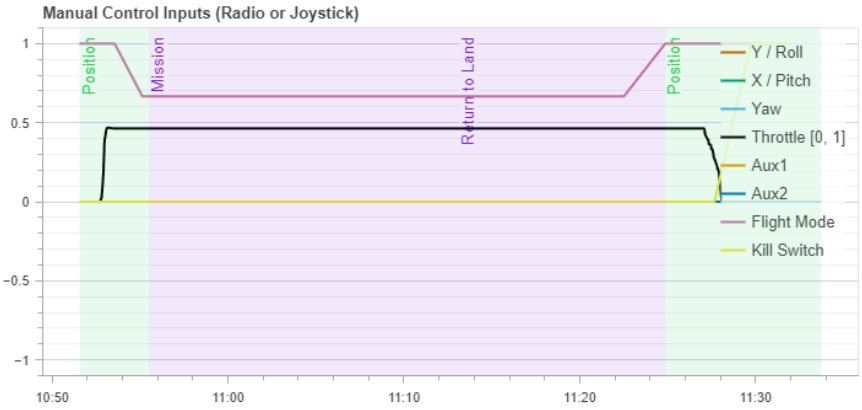


Figure 3 – Control Inputs during Fully Autonomous Flight

Table 1 presents the results we obtained for each of the four experiments with the measured RMSE presented in millimeters. In Experiment 1, where the localization was solely based on the 3D LIDAR in conjunction with SLAM, this showed the highest RMSE as expected. In Experiment 2, where the 1D downward-facing LIDAR was utilized for the height measurement, a significant improvement can be observed, which is expected as the error accumulates in the z-direction in Experiment 1 due to the noise which is large at takeoff due to higher speeds. This demonstrated that a two sensor solution provides better accuracy. The error in the x and y directions remained almost unchanged which is expected as the position information in those two dimensions still solely relies on the position data coming from the 3D LIDAR SLAM. In Experiment 3, a Kalman Filter was applied to combine both LIDAR sensors measurements in the z-direction and its prediction features, the accuracy in the x-y-plane improved significantly, by lowering the difference between the two adjacent localization measurements which previously caused higher overall movement of the UAV. Further and significant improvement was observed in Experiment 4 when the covariance matrices of the Kalman Filter adapted to the vibration on the UAV. IMU data was also added as a control input. This improvement was especially noticeable during takeoff and rapid position changes, vibration effects the localization causing inaccuracies that are present for the remainder of the flight. The data demonstrates that

by adding sensor technology and increasing the systems intelligence we were able to significantly reduce the observed error with respect to the ground truth data in all three dimensions. Specifically, error in the z-direction is almost one-fourth of the first test case while the error in the horizontal x-y plane is reduced by approximately fifty percent.

Table 1 – RMSE Ground Truth vs Measured Data

	RMSE in mm		
Experiment Description	x	y	z
Experiment 1: 3D LIDAR	148.1	131.1	214.5
Experiment 2: 3D + 1D LIDAR	166.6	154.0	50.6
Experiment 3: Kalman Filter	92.6	98.1	54.8
Experiment 4: Adaptive Kalman Filter	81.5	61.6	55.2

The position estimate obtained from the test case of our proposed approach and motion capture measurements are depicted in Fig. 4 for the x-axis, in Fig. 5 for the y-axis, and in Fig. 6 for the z-axis with respect to time of flight. These figures collectively provide a detailed representation of the UAVs trajectory across a three-dimensional space utilizing the Adaptive Kalman Filter estimation scheme. Fig. 6 also demonstrates how our proposed method of fusing both LIDAR sensors helps to smoothen the measurements from the distance sensor (1D LIDAR) that is used as the main reference point, which contributes to a flight with less correction of the UAV and smoother trajectory.

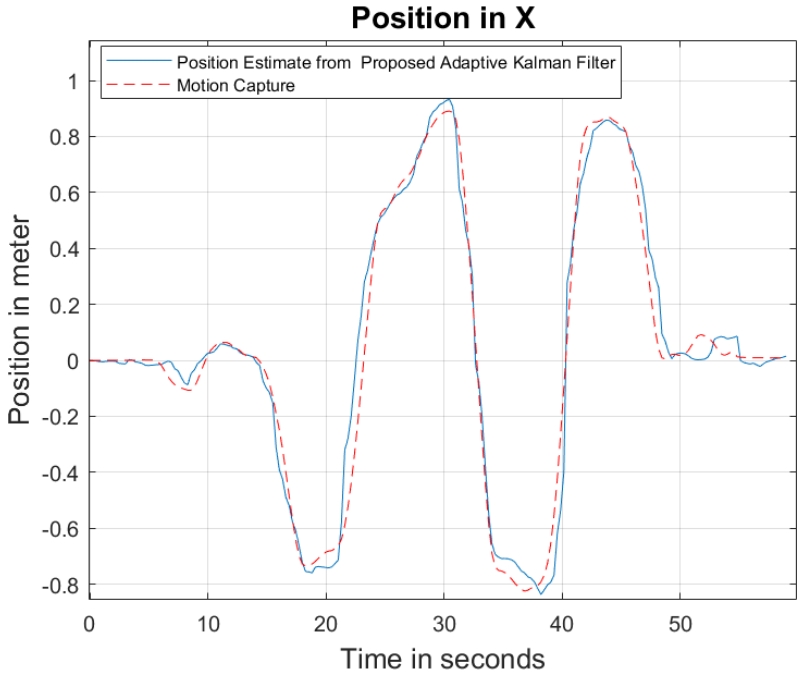


Figure 4 – Localization W.R.T. the x-axis

Overall, the proposed system provides accurate localization with respect to the size of the UAV itself and the feature-poor environment, which traditionally is challenging for LIDAR sensors. The LIDAR-based approach enables adaptability across a wide range of environments, while the AKF scheme provides runtime assurance by compensating for noise and inconsistencies in sensor data..
While it is difficult to compare the results of our proposed method to other approaches available in literature due to the differences in the UAV itself and the experiment setup, we were able to provide significantly higher position estimate accuracy during flight compared to visual inertial approaches. As shown in Table 2, in [11] for example, a drift of 400 millimeters in x and 1700 millimeters in y was reported during hover flight test. In [12], while the reported error for hover test were smaller

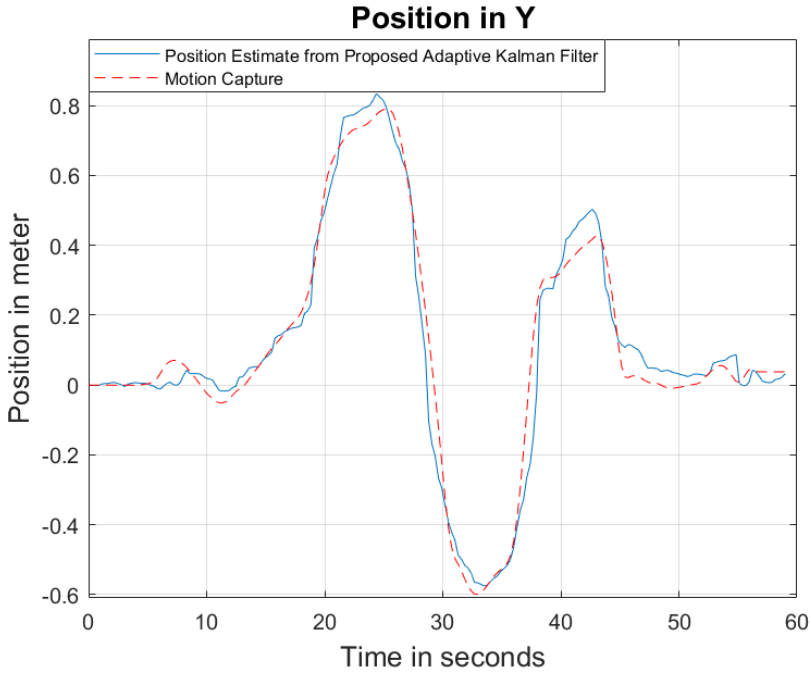


Figure 5 – Localization W.R.T. the y-axis

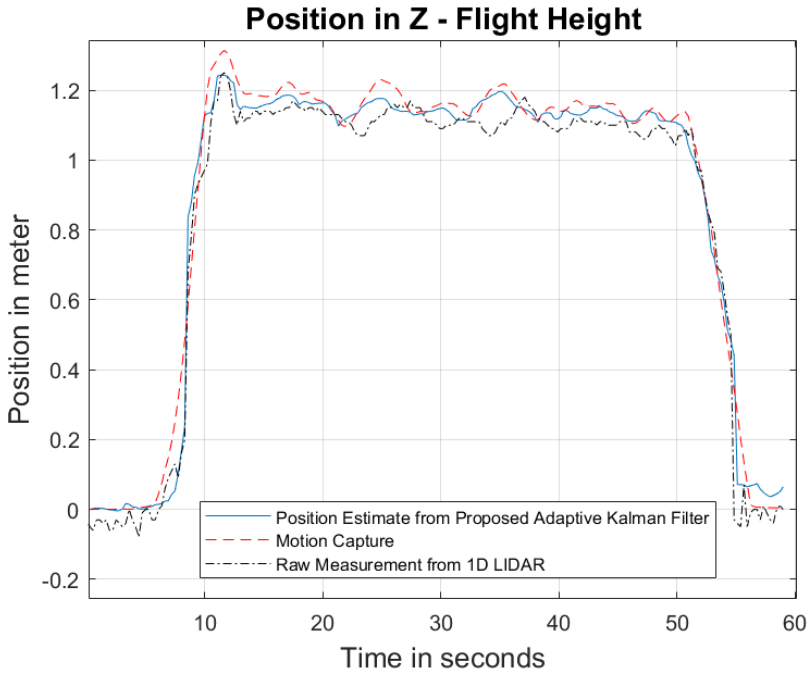


Figure 6 – Localization W.R.T. the z-axis

as compared to ours (which is expected since ours was square pattern flight), the reported errors in square patterns were much higher than ours in the x and y directions.
Here, it must also be noted that their test results were achieved utilizing a significantly smaller microdrone with a size of $\approx$ 150 millimeters. In [6], the reported RMSE values in the x-y plane and the z-direction are notably higher than those observed in our experiments. While it must be considered that their UAV tests were conducted over longer duration and greater distance, which may contribute to these discrepancies, the presented error over time in each x-, y-, and z-dimension were consistently showing errors of this extent.

Table 2 – RMSE Results Reported In Existing Literature

	RMSE in mm		
Experiment Description	x	y	z
Hover Test in [11]	400	1700	not reported
Hover Test in [12]	51.9	42.8	39.0
Square Pattern Indoor Flight in [12]	161.9	142.8	21.5
Square Pattern Indoor Flight in [6]	289		268

5. Conclusion

In this paper, we presented a novel approach to localize a UAV in GPS-denied environments in real-time by utilizing onboard sensors in an adaptive filtering framework. We developed a Kalman Filter based adaptive sensor fusion scheme that combined data from a 3D LIDAR and 1D LIDAR distance sensor and corrected for estimation inaccuracies caused by excessive vibration on the system for runtime assurance. We successfully demonstrated that our UAV was able to accurately estimate its location in space by calculating the RMSE to the ground truth which was obtained from a highly precise OptiTrack Motion Capture system. We also showed that our algorithm and choice of sensors improved the accuracy significantly. Utilizing our proposed approach we were able to reduce the error to 81.5 millimeters in the x-direction, 61.6 millimeters in the y-direction, and 55.2 millimeters in the z-direction. Considering the size of our UAV and its lifting capabilities, we demonstrated an efficient and accurate position estimation framework while also comparing it to other methods that are currently available. The developed system shows its capability to support fully autonomous indoor flight, smooth transition from outdoor to indoor environments, and thus presents a viable platform for telehealth applications within residential settings.

Future work involves including other sensory modalities such as vision and ultrasound that would improve the estimation and make it more robust to varying environmental conditions. Additionally, the introduction of automating the optimization process of obtaining the vibration parameters is a future direction of this work to allow simple and fast transferability to various UAV platforms.

6. Acknowledgments

This research was supported by the National Science Foundation (NSF) under grant number 2234561.

7. Contact Author Email Address

Luke Busse:
busselu@mail.uc.edu
3080 Exploration Ave, 45206 Cincinnati, OH, USA

8. Copyright Statement

The authors confirm that they, and/or their company or organization, hold copyright on all of the original material included in this paper. The authors also confirm that they have obtained permission, from the copyright holder of any third party material included in this paper, to publish it as part of their paper. The authors confirm that they give permission, or have obtained permission from the copyright holder of this paper, for the publication and distribution of this paper as part of the ICAS proceedings or as individual off-prints from the proceedings.

References

[1] Navid Kayhani, Adam Heins, Wenda Zhao, Mohammad Nahangi, Brenda McCabe, and Angela Schoellig. Improved Tag-based Indoor Localization of UAVs Using Extended Kalman Filter. In *Proceedings of the 36th International Symposium on Automation and Robotics in Construction (ISARC)*, pages 624–631. International Association for Automation and Robotics in Construction (IAARC), 2019.

[2] Eduard Mráz, Jozef Rodina, and Andrej Babinec. Using fiducial markers to improve localization of a drone. In *2020 23rd International Symposium on Measurement and Control in Robotics (ISMCR)*, pages 1–5. IEEE, 2020.

[3] Gennaro Ariante, Salvatore Ponte, and Giuseppe Del Core. Bluetooth Low Energy based Technology for Small UAS Indoor Positioning. In *2022 IEEE 9th international workshop on metrology for AeroSpace (MetroAeroSpace)*, pages 113–118. IEEE, 2022.

[4] Alireza Famili, Angelos Stavrou, Haining Wang, and Jung-Min Park. PILOT: High-Precision Indoor Localization for Autonomous Drones. *IEEE Trans. Veh. Technol.*, pages 6445–6459, 2023.

[5] Janis Tiemann and Christian Wietfeld. Scalable and precise multi-UAV indoor navigation using TDOA-based UWB localization. In *2017 international conference on indoor positioning and indoor navigation (IPIN)*, pages 1–7. IEEE, 2017.

[6] A Masiero, F Fissore, R Antonello, A Cenedese, and A Vettore. A COMPARISON OF UWB AND MOTION CAPTURE UAV INDOOR POSITIONING. *The International Archives of the Photogrammetry, Remote Sensing and Spatial Information Sciences*, 42:1695–1699, 2019.

[7] Kheireddine Choutri, Mohand Lagha, Souham Meshoul, Hadil Shaiba, Akram Chegrani, and Mohamed Yahiaoui. Vision-Based UAV Detection and Localization to Indoor Positioning System. *Sensors*, 24(13):4121, 2024.

[8] Gustavo Gargioni, Marco Peterson, JB Persons, Kevin Schroeder, and Jonathan Black. A Full Distributed Multipurpose Autonomous Flight System Using 3D Position Tracking and ROS. In *2019 International Conference on Unmanned Aircraft Systems (ICUAS)*, pages 1458–1466. IEEE, 2019.

[9] Péter Troll, Károly Szipka, and Andreas Archenti. Indoor Localization of Quadcopters in Industrial Environment. In *SPS2020*, pages 453–464. IOS Press, 2020.

[10] Heng Deng, Usman Arif, Kun Yang, Zhiyu Xi, Quan Quan, and Kai-Yuan Cai. Global optical flow-based estimation of velocity for multicopters using monocular vision in GPS-denied environments. *Optik*, 219:164923, 2020.

[11] Seyed Jamal Haddadi and Eugenio B Castelan. Visual-Inertial Fusion for Indoor Autonomous Navigation of a Quadrotor Using ORB-SLAM. In *2018 Latin American Robotic Symposium, 2018 Brazilian Symposium on Robotics (SBR) and 2018 Workshop on Robotics in Education (WRE)*, pages 106–111. IEEE, 2018.

[12] Xu Zhang, Bin Xian, Bo Zhao, and Yao Zhang. Autonomous Flight Control of a Nano Quadrotor Helicopter in a GPS-denied Environment Using On-Board Vision. *IEEE Transactions on Industrial Electronics*, 62(10):6392–6403, 2015.

[13] Peide Wang. Research on comparison of lidar and camera in autonomous driving. In *Journal of Physics: Conference Series*, volume 2093, page 012032. IOP Publishing, 2021.

[14] Václav Pritzl, Matouš Vrba, Petr Štěpán, and Martin Saska. Cooperative Navigation and Guidance of a Micro-Scale Aerial Vehicle by an Accompanying UAV using 3D LiDAR Relative Localization. In *2022 International Conference on Unmanned Aircraft Systems (ICUAS)*, pages 526–535. IEEE, 2022.

[15] Chenming Xin, Guoyou Wu, Congyu Zhang, Kai Chen, Jinjian Wang, and Xiang Wang. Research on Indoor Navigation System of UAV Based on LIDAR. In *2020 12th International Conference on Measuring Technology and Mechatronics Automation (ICMTMA)*, pages 763–766. IEEE, 2020.

[16] Derek Chen and Grace Xingxin Gao. Probabilistic graphical fusion of LiDAR, GPS, and 3D building maps for urban UAV navigation. *Navigation*, 66(1):151–168, 2019.

[17] Matěj Petrlík, Tomáš Krajník, and Martin Saska. LIDAR-based Stabilization, Navigation and Localization for UAVs Operating in Dark Indoor Environments. In *2021 International Conference on Unmanned Aircraft Systems (ICUAS)*, pages 243–251. IEEE, 2021.

[18] Wei Gao, Jingchun Li, Guangtao Zhou, and Qian Li. Adaptive Kalman Filtering with Recursive Noise Estimator for Integrated SINS/DVL Systems. *J. Navigation*, pages 142–161, 2015.

[19] Young Soo Suh. Orientation estimation using a quaternion-based indirect Kalman filter with adaptive estimation of external acceleration. *IEEE Transactions on Instrumentation and Measurement*, 59(12):3296–3305, 2010.

[20] Dongjiao He, Wei Xu, Nan Chen, Fanze Kong, Chongjian Yuan, and Fu Zhang. Point-LIO: Robust High-Bandwidth Light Detection and Ranging Inertial Odometry. *Advanced Intelligent Systems*, 5(7):2200459, July 2023.